Order—disorder transitions in polytetrafluoroethylene

J. J. Weeks, I. C. Sanchez, R. K. Eby
Polymer Science & Standards Division, National Bureau of Standards, Washington, DC 20234, USA
and C. I. Poser
Polymer Science and Engineering Department, University of Massachusetts, Amherst, MA 01003, USA
(Received 7 November 1979)

The phase diagram of polytetrafluoroethylene is enlarged by differential scanning calorimetry to include the concentration of hexafluoropropylene comonomer units. The two transitions near 292 and 303 K in the homopolymer move to lower temperatures and apparently become one at small concentrations. Analysis of the data yields 295 K for the temperature and 13.2 J/g for the heat of transition of an infinitely large homopolymer crystal. The heat of transition associated with the formation of a crystal defect is 0.021 eV. The qualitative features of the transition can be accounted for by a mean-field model which involves two order parameters corresponding to planar units and helix reversals. This model yields two transitions which move closer together and to lower temperatures with increasing comonomer concentration. Decreasing lamella thickness will have a qualitatively similar effect.

INTRODUCTION

Polytetrafluorethylene exhibits a phase diagram with four solid phases and the melt[1]. At one atmosphere, melting occurs near 600 K and solid--solid crystal transitions near 292[2] and 303 K[3–4]. The latter affect the specific volume[5,6] dielectric constant[7], heat capacity[8], n.m.r. spectrum[9], modulus of longitudinal ultrasonic waves[10], and spectroscopic properties[11] of the polymer. In the low temperature phase, the crystal is well ordered in a structure which is probably triclinic[12]. At 292 K, the structure changes to hexagonal and the structure develops some disorder which arises from a mechanism that rotates the atoms about the molecular axis. This mechanism keeps the molecular axis unchanged. At 303 K, the hexagonal cell dimensions increase and the disorder increases corresponding to an increased angle of rotation of the atoms about the molecular axis[12]. The main mechanisms of rotation which have been proposed are the introduction of reversals of the hand of the helical molecules and planar zig-zag units[11,13–18].

In this article, the phase diagram for these transitions is extended to include the concentration of hexafluoropropylene units in copolymers of tetrafluoroethylene (TFE) and hexafluoropropylene (HFP). Previous measurements have shown the systematic influence of the concentration of these units on the melting temperature[19] but, the solid–solid transition has been observed at only one comonomer concentration[20]. The present data were obtained by differential scanning calorimetry (DSC) for comonomer concentrations covering a range of 0 to approximately 6.9 CF_3 branches per hundred main–chain carbon atoms. Thermodynamic information about the transition in copolymers is determined from the DSC data. A model of the order–disorder transitions is developed and solved numerically. There have been earlier attempts at developing such a model. One[21], which had only one order parameter, led to aphysical results because an unrealistic energy representation was adapted. A more recent effort has the formal possibility of including more than one disordering mechanism[22]. However, this was not pursued and the effects of coupling between the mechanisms was not observed. The present theory is a mean-field model which involves two order parameters. It yields two transitions over some ranges of the parameters and one in others. It also exhibits results in qualitative agreement with experimental observations of the effect of parameters such as comonomer concentration. Aspects of both the experimental and theoretical work have been reported previously[23].

EXPERIMENTAL

Random copolymers of TFE with HFP[19,20] were crystallized from the melt to produce the samples. Long periods of most had been measured previously by small-angle X-ray diffraction[19] and those for the new samples were measured in the same manner. Comonomer concentration values, X, which had been provided by the manufacturer and others which have been estimated by interpolation of unit cell dimensions[19] were revised according to improvements in the analytical methods[24]. For those samples used previously, the sample numbers are those given in reference 10. The molecular weights, M_n, of the copolymers varied from 5.2×10^4 to 2.6×10^5, implying two or more folds per molecule for the long periods observed. The polytetrafluoroethylene molecular weight was an order of magnitude greater.

The specific heats were measured in the range of ~100–400 K using a scanning calorimeter (DSC–2)[25]. The samples were run against a sapphire reference of nearly equal heat capacity (52 mJ/K at 300 K) on a sensitive range (4.18 or 8.36 mJ/s) and usually at a heating rate of 10 K/min. By replacing the sample with another sapphire standard of similar weight and rerunning under the same conditions, the sample specific heat could be calculated from the difference

0032–3861/80/030325–07$02.00

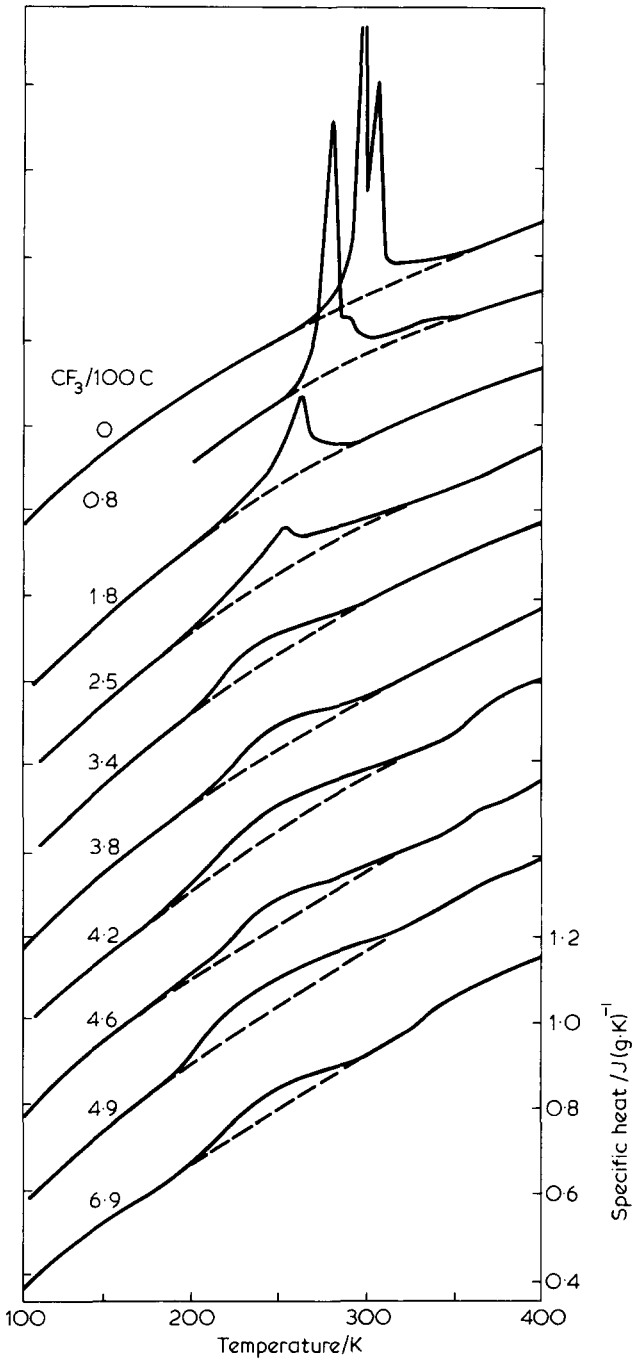

Figure 1 Specific heat, C_p, as a function of temperature (heating) and comonomer concentration. The scale at right applies to the sample with 6.9 CF_3/100C. Each succeeding curve is displaced vertically by 0.2 J(gK)

in power displacements together with the known specific heat of sapphire[26]. Usually an interval of 50 degrees was scanned before stopping to record the isothermal baseline. Displacements were measured from a linear interpolation of these baselines. The instrumental calibration of the power was made by scanning a sample of gold over the range of interest using 30 K intervals. The displacement sensitivity was found to be only slightly temperature dependent, increasing by 1% in 118 degrees. Scanning rate and recorder chart drive speed were well correlated and required no correction.

Temperature corrections for the scale reading and for scanning lag were made according to published recommendations[27]. The equilibrium scale corrections were obtained from the solid–solid transition (at 122.4 K) in cyclopentane and the melting transitions of n-heptane, n-octane, water, *p*-nitrotoluene, and indium metal. Corrections at other temperatures were obtained from an interpolation formula. The estimated uncertainty of the polymer sample temperature is 1–2 degrees which considers both the repeatability of the standards and the appreicable gradient across the sample.

EXPERIMENTAL RESULTS AND DISCUSSION

The specific heats, C_p, of representative samples are shown in *Figure 1*, where each curve is displaced vertically by 0.2 J/(gK). Backgrounds were drawn under the transition peaks by extrapolating with a smooth curve from below and above the transition region. These were subtracted from the C_p curves to give the typical peaks shown in *Figure 2*. The area under such curves is taken as the transition heat, Δh_t, and the corrected[27] peak temperature as the transition temperature*. Note that for $X > \sim 1$ only one transition can be resolved.

Several heating and cooling rates were used to yield the results given in *Table 1*. Any correlation between transition temperature and rate[3] is apparently masked by experimental errors in the present measurements. Therefore, only the rate of 10 K/min was used to obtain the results given in *Table 2*. For all the samples, the average difference between the heating and cooling transition temperatures is 0.8K. This value is subject to a 2K standard deviation which is primarily a result of the very broad nature of the transition and uncertainty in the background. Hence, the average of the heating and cooling results is used as the estimated transition temperature. (This assumes that the small hysteresis effects are equal for heating and cooling). Similarly, the heating and cooling results for the heat of transition differed little and the average is given in *Table 2*.

* The small endotherms near 330 K are associated with the glass transition and depend on annealing time as well as the amorphous fraction

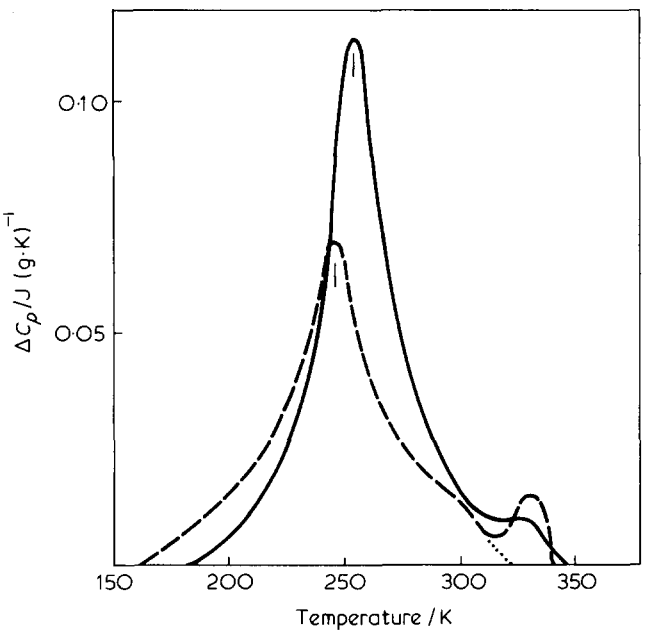

Figure 2 Typical curves obtained by subtracting backgrounds such as those shown in *Figure 1*. The area under these curves is taken as the heat of transition. The upper curve (A) is for sample 2A and the lower (B) for 2Q of *Table 2*. Both are for data obtained during heating

In order to investigate the effect of crystallinity on the heat of transition, sample 2 was prepared in three forms (sample 2A, 2 and 2Q of *Table 2*) by changing the rate of cooling from the melt. The results for 2A and 2Q are the ones shown in *Figure 2*. Clearly, the transition is associated with the crystals just as it is in the homopolymer. Thus, the phase diagram of polytetrafluoroethylene can be enlarged to encompass CF_3 concentration as shown in *Figure 3*. As noted, phase IV can be resolved only for small concentrations and thus appears to exist over only a narrow range of temperature, pressure[16], and composition. X-ray diffraction[23] shows that the structure of both the high temperature phase I and the low temperature phase II of the copolymer are similar to those of the homopolymer, except that CF_3 groups introduce a longitudinal disorder which gradually increases with their concentration. X-ray diffraction also shows only one transition for higher concentrations of CF_3 groups. At the transition, the observed changes in long period (~5%) are within the limits of experimental error. The high pressure phase III of the homopolymer is modified by the rotational disorder introduced by the CF_3 groups in the copolymer[28].

The average transition temperatures were found empirically to depend on the parameters of the model to be presented: copolymer composition and long period, l, modified by the degree of crystallinity, χ. Fitting the data yielded the following equation:

$$T_t = 295 \pm 1 - (20 \pm 2)X + (3.5 \pm 0.6)X^2 - (0.21 \pm 0.06)X^3 - (304 \pm 68)(1/\chi l) + (1273 \pm 360)(1/\chi l)^2 \quad (1)$$

The standard deviation is 1.7 K, which is comparable to the experimental value. This fit yields 295 K as the transition temperature of an infinitely large perfect crystal. *Figure 4* is a more detailed plot of transition temperatures *versus* composition than that given in *Figure 3* and shows the

Table 1 Effect of scanning rate on the peak transition temperature

Sample	Comonomer* concentration	Long period (nm)	Scanning rate (deg/min)	Transition temperature, K† Heating	Cooling
20‡	0	600 est.	1.25	296.2	293.3
	0	600 est.	2.5	296.1	291.9
	0	600 est.	10	294.0	292.8
1	1.8	51	0.62	257.7	257.4
	1.8	51	5	258.5	255.8
	1.8	51	10	258.0	256.8

* CF_3 per 100 main-chain carbon atoms
† For the lower temperature transition of sample 20 and the only resolved transition of sample 1
‡ The sample used in reference 16 of the maint text

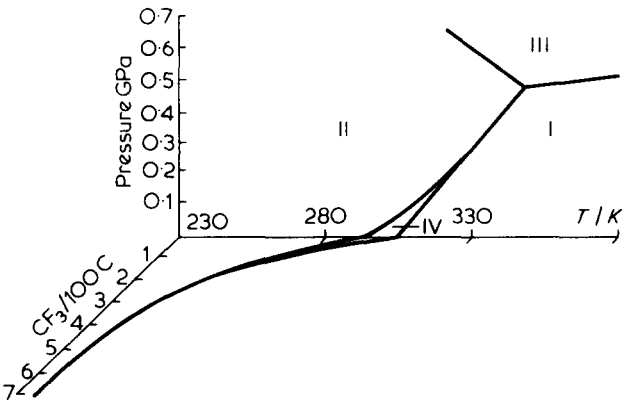

Figure 3 Phase diagram for TFE–HFP copolymers

Table 2 Transition temperatures, heats of transition and sample characteristics

Sample number	Comonomer* concentration	Long period (nm)	Transition temperature, K† Heating	Cooling	Average	Heat of transition (J/g)	Degree of crystallinity
20‡	0	600 est.	294.0	292.8	293.4	11.01	78
21	0	92	290.5	285.4	288.0	5.82	41
14	0.8	50	277.7	275.1	276.4	7.11	67
1	1.8	51	258.0	256.8	257.4	5.75	52
2A	2.5	59	255.0	252.7	253.8	5.24	36
2	2.5	50	248.1	247.1	247.6	3.44	30
2Q	2.5	34	246.8	244.5	245.6	3.72	29
3A	3.4	41	245.2	244.0	244.6	3.43	33
3	3.4	36	241.4	239.6	240.5	2.89	28
15	3.4	21	244.6	243.6	244.1	4.39	31
4	3.8	53	244.8	245.6	245.2	3.85	40
5	3.8	48	244.2	242.6	243.4	3.92	38
16	3.8	37	242.7	241.6	242.2	2.97	31
6	3.8	40	245.6	243.8	244.7	5.63	40
40	3.8	29	234.6	239.8	237.2	3.39	29
7	4.2	35	238.2	239.2	238.7	4.44	31
8	4.6	45	244.3	244.1	244.2	4.10	34
9	4.6	41	241.4	241.2	241.3	4.14	35
10	4.6	35	240.8	242.2	241.5	4.14	33
10Q	4.6	27	236.0	238.3	237.2	3.06	31
11	4.9	34	239.8	238.9	239.4	3.47	25
23	6.9	32	238.0	236.0	237.0	2.21	24

* CH_3 per 100 main-chain carbon atoms
† For the lower temperature transition of samples 20 and 21 and the only resolved transition of the copolymer samples
‡ The sample used in reference 16 of the main text

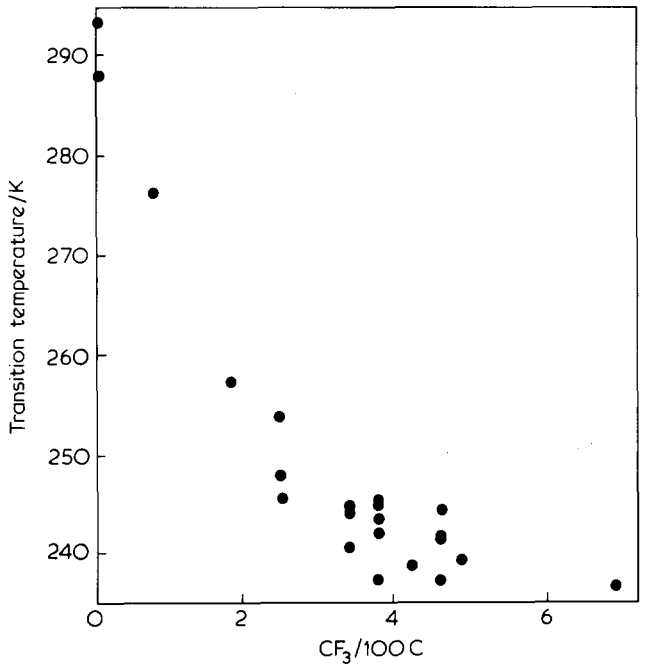

Figure 4 Average transition temperature as a function of CF_3 concentration

general non-linear nature as well as the χ dependence at constant X. The higher order terms could arise from the model to be presented. However, they might also arise either from the interaction of the defects at higher concentrations, or from preferential rejection of the comonomer units at higher concentrations. (i.e., the comonomer unit concentration in the crystal, X_c, is unequal to X. In this article, we assume $X_c = X$.)

If one assumes in parallel with the model to be presented that the heat of transition decreases linearly with X and is independent of temperature, one can write the following expression for the observed heat of transition, Δh_t, of a copolymer crystal:

$$\Delta h_t/\chi = \Delta H_t^0 (1 - AX) \qquad (2)$$

In this equation, ΔH_t^0 is the heat of transition of an infinitely large homopolymer crystal. The factor A represents the ratio of the heat of transition associated with the formation of a crystal defect to ΔH_t^0. The heat of fusion of the present samples was measured and used in an equation analogous to equation 2[29] to yield the values of χ given in *Table 2*. The greatest observed value of 72.3 J/g for an unsintered sample of the homopolymer was used as the heat of fusion of an infinitely large homopolymer crystal. The previously determined[29] effect of the comonomer units was used after correction for the revised comonomer concentrations[24] and the relatively smaller effect of the fold surface was neglected. Fitting equation 2 to $\Delta h_t/\chi$ and X yields:

$$\Delta h_t/\chi = (13.2 \pm 0.9)(1 - 2.8X) \qquad (3)$$

The standard deviation is 1.7 J/g and the maximum deviation is 2.8 J/g. The value of 13.2 ± 0.9 J/g for ΔH_t^0 agrees reasonably well with estimates which can be made on the basis of measurements of the homopolymer[8,16,21,30,31]. The value 2.8 corresponds to ~0.02eV per defect or 0.45 kcal/mol of defects, a result which is of the same order as that for the melting transition[29] (after correction for the revised[24] comonomer concentrations). On the basis of an elastic model for the defect energy[19], it is plausible that this is of the same order as the defect energy of the melting transition. In the elastic model, the defect energy depends on the shear modulus and the change of that modulus from phase II to phase I is of the same order as that from phase I to the melt[32]. Of course, some caution must be exercised in attempting to account for the defect transition energy on the basis of an elastic model. Also note that the value, 2.8, is subject to uncertainty not only from the fitting but also from the background uncertainties in curves with such small heats of transition as those in *Figure 1*.

THEORY

As mentioned previously, there is a body of experimental evidence that indicates that the solid–solid transitions in polytetrafluoroethylene near 292 K and 303 K are associated with increased rotational disorder around the molecular axis[11–18]. A small rotation of a helical monomer unit can convert that unit to a planar unit; a larger rotation can reverse the helical sense of the unit. The simple model which is presented below allows a helical unit to be converted to a planar unit or to change its helical sense.

A polytetrafluoroethylene lamellar crystal is idealized as an assembly of N rodlike molecules each containing n monomer units which occupy nN sites of a lattice. Each monomer unit can exist in a right-handed helical, left-handed helical, or planar state. When all nN units are in right- or left-handed helical states, the crystal is in its ground state. Introduction of planar or helical units of opposite sense will raise the potential energy of the crystal.

The total number of monomer–monomer pair interactions in the crystal is $znN/2$ where z is the coordination number of the lattice. The four types of pair interactions and their energies, ϵ_i, are shown in *Table 3*. Although there are both intra- and intermolecular interactions, these will be represented by an average value in what follows. The formally complete expression can be recovered by replacing $z\epsilon_1$ by $(z_{\text{inter}}\epsilon_{\text{inter}} + z_{\text{intra}}\epsilon_{\text{intra}})$ etc. in the equations to be derived.

In the mean field approximation, the probability (joint) of an i, j pair is equal to X_iX_j where the X's are mole fractions. In this approximation, the potential energy (E) of the crystal relative to the ground state is

$$E = (znN/2)[X_p^2\epsilon_1 + 2X_p(X_R + X_L)\epsilon_2 + 2X_RX_L\epsilon_3] \qquad (4a)$$

$$X_p + X_R + X_L = 1 \qquad (5)$$

where X_p, X_R and X_L are the mole fractions of planar, right-handed helical, and left-handed helical units, respectively.

One of the concentration variables can be eliminated by introducing order parameters α and β:

Table 3 Types of pair interactions and their relative energies

Interaction*	Energy
RL	ϵ_3
RP or LP	ϵ_2
PP	ϵ_1
RR or LL	0

* R ≡ right handed helical unit, L = left handed helical unit, and P ≡ planar unit

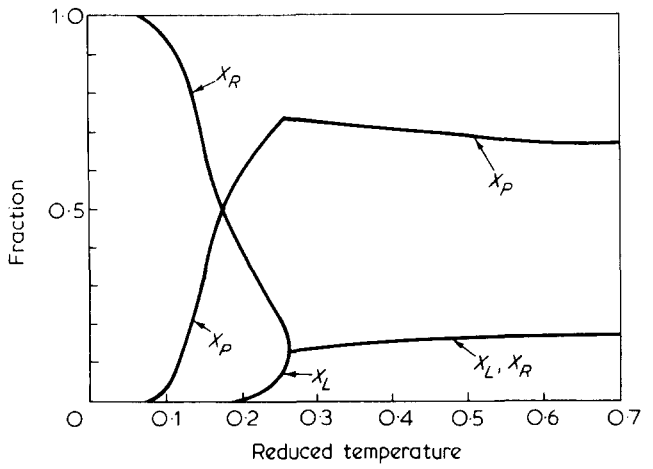

Figure 5 Fraction of right-handed, X_R, left-handed, X_L, and planar units, X_p, as a function of the reduced temperature. The values of σ_1, σ_2 and q are 0.2, 0.21 and 3, respectively

$$X_p \equiv \beta; X_R - X_L \equiv \alpha \tag{6}$$

$$X_R = (1 + \alpha - \beta)/2 \tag{7}$$

$$X_L = (1 - \alpha - \beta)/2 \tag{8}$$

Now, assuming $\epsilon_3 \neq 0$, the potential energy can be expressed as

$$E = (znN\epsilon_3/2)\{\beta^2\sigma_1 + 2\beta(1-\beta)\sigma_2 + [(1-\beta)^2 - \alpha^2]/2\} \tag{4b}$$

where

$$\sigma_1 \equiv \epsilon_1/\epsilon_3 \text{ and } \sigma_2 \equiv \epsilon_2/\epsilon_3 \tag{9}$$

The configurational partition function for the crystal is

$$Z = \sum_{\alpha,\beta} \Omega(\alpha,\beta)\exp[-E(\alpha,\beta)/kT] \tag{10}$$

where Ω is the number of configurations available to the crystal for a given value of (α, β) and kT has its usual significance. The sum is over all possible values of α and β, but as is customary we replace the sum by its maximum term. This procedure is equivalent to equating the Helmholtz free energy, $A = -kTlnZ$, to the generic term in the partition function and then minimizing the free energy with respect to α and β:

$$\left(\frac{\partial A}{\partial \alpha}\right)_\beta = 0 \text{ and } \left(\frac{\partial A}{\partial \beta}\right)_\alpha = 0 \tag{11}$$

The number of configurations Ω available to N_p planar units, N_R right-handed helical units, and N_L left-handed helical units is a trinomial coefficient:

$$\Omega = q^{N_p}\frac{(nN)!}{N_p!\,N_R!\,N_L!} \tag{12}$$

or

$$ln\Omega = -nN[X_p lnX_p + X_R lnX_R + X_L lnX_L - X_p lnq] \tag{13}$$

where q is the degeneracy of a planar state relative to a helical state. Lattice models with degenerate states are commonly referred to as Potts models[33]. Recently, there has been an upsurge of interest in Potts models because they appear to exhibit a first order phase transition in three dimensions for $q > 3$[34–36]. Physically, what is implied by $q > 1$ for the present system is that the entropy of a planar state is greater than that of a helical state, or equivalently, the 'width' of the potential energy well of a planar state is larger than that of a helical state.

Minimization of the free energy yields the following equations for α and β:

$$\beta = 1 - \alpha\coth(\alpha/\tilde{T}) \tag{14}$$

$$\alpha^2 = (1-\beta)^2 - (2\beta/q)^2 \times \exp\left\{\frac{2}{\tilde{T}}[(\beta-1) + 2\beta\sigma_1 + 2(1-2\beta)\sigma_2]\right\} \tag{15}$$

where $\tilde{T}$ is a dimensionless or reduced temperature defined by

$$\tilde{T} = kT/(z\epsilon_3/2) \tag{16}$$

Note that these equations are satisfied by the physically correct values of α and β at low and high temperatures. Thus, at low temperatures there are molecules in either the left- or right-handed state only ($\alpha = \pm 1$ and $\beta = 0$). At high temperatures, all states including the q degerate planar ones are equally populated ($\alpha = 0$ and $\beta = q/q + 2$).

COMPUTATIONAL RESULTS AND DISCUSSION

Figure 5 depicts a typical behaviour of X_p, X_R, and X_L (resulting from the behaviour of α and β) as a function of temperature. Arbitrary values of $\sigma_1 = 0.20$, $\sigma_2 = 0.21$ and $q = 3$ were chosen. As a function of $\tilde{T}$, the fractional content of the various units proceeds in three stages. At low values of $\tilde{T}$, all are in the same helical state, in this case the right-handed one. As $\tilde{T}$ increases some of the right-handed units are transformed into planar units. A further increase in $\tilde{T}$ results in the appearance of left-handed helical units. Finally a discontinuity occurs in the equations after which X_R and X_L are equal and slowly increase while X_p decreases slowly to the high temperature equilibrium values. The assumption of an initially all left-handed state does not change the results.

Figure 6 shows the heat capacity curve corresponding to the parameters in *Figure 5*. (The heat capacity, $\partial E/\partial T$, is reduced by nNk. Comparison of the two figures shows the correspondence of the peak in the heat capacity curve to the rapid conversion of helical units to planar units. The increase in the heat capacity preceding the discontinuity is associated with the appearance of left-handed helical units, and the discontinuities in the two figures correspond exactly. The first peak in the heat capacity is associated with a planar transition, while the second one is caused by helix reversals.

The word 'transition' is used loosely here. For the set of σ_1, σ_2, and q used in *Figures 5* and *6*, the first transition is neither first nor second order whereas the second transition is second order (finite discontinuity). So, although *Figure 6*

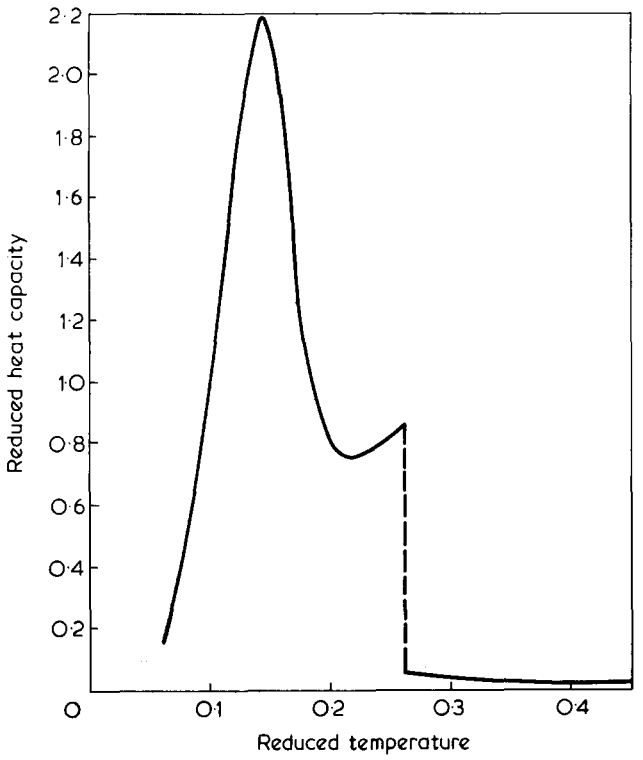

Figure 6 Reduced heat capacity corresponding to the fractions in *Figure 5*

appears qualitatively similar to the experimental heat capacity curve, the similarity is not exact because the experimentally observed transition at 292 K is generally believed to be first order. However, the similarity becomes stronger as q is allowed to increase because the transition begins to take on the character of a first order phase transition. *Figure 7* illustrates the effect of q on the shape of the heat capacity curve. Increasing q increases the peak height of the first transition markedly and decreases the height of the second transition in a less pronounced manner. Large values of q also move the two transitions closer together in temperature.

It is not necessary for $\sigma_1 \neq \sigma_2$ to observe two transitions; if $\sigma_1 = \sigma_2$, two transitions are still obtained when σ_1 and σ_2 are sufficiently small. The important condition for the observation of two transitions is that the energy differences $|\epsilon_3 - \epsilon_1|$ and $|\epsilon_3 - \epsilon_2|$ be large. This ensures good separation between the planar and helix reversal states. (Note that if σ_1 and σ_2 are relatively large compared to unity, the reversal transition will precede the planar one.) If the energies are not sufficiently separated, the two transitions couple into one. One transition results for rather wide ranges of the parameters in the present model. Unfortunately, because of computational difficulties, the equations cannot be solved for values of the parameters which would move the two transitions close enough together to yield the experimentally observed ratio of the homopolymer transition temperatures of 1.04.

GENERALIZATION OF MODEL TO COMONOMER UNITS

The model can be generalized easily to include comonomer units. Let X equal the mole fraction of co-units (e.g. CF_3) so that

$$X_p + X_R + X_L + X = 1 \tag{17}$$

Each co-unit is assumed to produce a defect in the crystal and the defect energy is denoted by ϵ_d. The concentration of co-units is assumed to be low enough so that defects can be considered to be isolated and defect-defect interactions can be ignored. In this case, a term equal to $X\epsilon_d$ must be added to equation 4 for the crystal potential energy and equation 12 becomes

$$\Omega = q^{N_p} \frac{(nN)!}{N_p!\, N_R!\, N_L!\, N_X!} \tag{18}$$

Since X is a constant, we can still describe the system in terms of the order parameters α and β and now

$$X_R = (1 - X + \alpha - \beta)/2 \tag{19}$$

$$X_L = (1 - X + \alpha - \beta)/2 \tag{20}$$

Minimization of the free energy with respect to α and β yields two equations similar to equations 14 and 15. The new α and β equations can be obtained from 14 and 15 by replacing unity everywhere in these two equations by 1–X. The defect energy ϵ_d does not appear.

Introduction of co-units into the model causes several changes in the calculated heat capacity curves as illustrated in *Figure 8*. Crystalline defects raise both the potential energy and entropy of the low temperature crystal. Consequently, transition temperatures are lowered and the heats of transition are reduced. Also, the two transitions move closer together.

The effects of co-units described above will be increased further by the increase of unit cell dimensions with comonomer concentration[20]. Qualitatively, the ϵ_1 associated with the various pair interactions will be reduced and the numbers of reversed and planar units, at any temperature will increase. Physically, this will result in a lowered transition temperature.

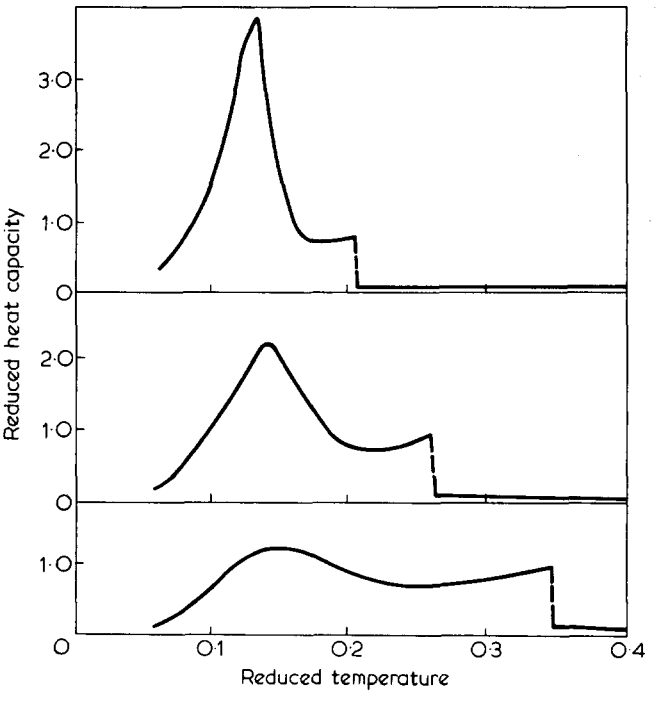

Figure 7 Reduced heat capacity for various values of planar state degeracy, q, with σ_1 and σ_2 equal to 0.2 and 0.21, respectively. (b) corresponds to *Figure 6* with q = 3; (a) q = 4; and for (c) q = 2

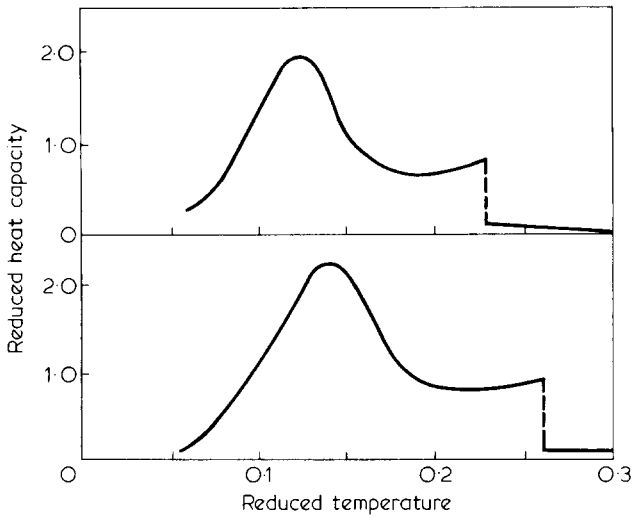

Figure 8 Reduced heat capacity for co-unit concentrations, X, of 0.1 (a) and 0 (b). The values of σ_1, σ_2, and q are 0.2, 0.21 and 3, respectively. (b) corresponds to *Figure 6*

The same effect will result from the increase of unit cell dimensions with decreasing lamella thickness[37]. In both cases, these effects are in qualitative agreement with the data in *Table 2.*

CONCLUSIONS

When the phase diagram of polytetrafluoroethylene is enlarged to encompass CF_3 concentration, the two solid–solid crystal transitions near 292 and 303 K move to lower temperatures and apparently become one at small concentrations. Thus, phase IV exists over only relatively small ranges of temperature, pressure and composition. Analysis of the data for the single transition yields 295 K for the temperature and 13.2 J/g for the heat of transition of an infinitely large homopolymer crystal. The heat of transition associated with the formation of a crystal defect is 0.02 eV.

The qualitative features of the solid–solid crystal transitions can be accounted for by an order–disorder model which contemplates the introduction of planar units and helix reversals as the disorders. A mean-field model which involves two order parameters yields two transitions over some ranges of the parameters. These transitions move closer together and to lower temperatures with increasing comonomer concentration. Decreasing lamella thickness will have a qualitatively similar effect. Pairs of other types of disorders (e.g., rotation of the molecular stem as a whole) would yield qualitatively similar results. More experimental work is needed to identify the disorders with more certainty.

REFERENCES

1 Matsushige, K., Enoshita, R., Ide, T., Yamauchi, N., Taki, S. and Takemura, T. *Jpn J. Appl. Phys.* 1977, **16**, 681
2 Rigby, H. A. and Bunn, C. W. *Nature* 1949, **164**, 583
3 Quinn, F. A., Jr., Roberts, D. E. and Work, R. N. *J. Appl. Phys.* 1951, **22**, 1085
4 Weir, C. E. *J. Res. Nat. Bur. Stand.* 1951, **46**, 207
5 Kirby, R. K. *J. Res. Nat. Bur. Stand.* 1956, **57**, 91
6 Beecroft, R. I. and Swenson, C. A. *J. Appl. Phys.* 1959, **30**, 1793
7 Koizumi, N., Yano, S. and Tsuji, F. *J. Polym. Sci.* 1968, **C23**, 499
8 Furakawa, G. T. McCoskey, R. E. and King, G. J. *J. Res. Nat. Bur. Stand.* 1952, **49**, 273
9 Slichter, W. P. *J. Polym. Sci.* 1957, **24**, 173
10 Eby, R. K. and Sinnott, K. M. *J. Appl. Phys.* 1961, **32**, 1765
11 Brown, R. G. *J. Chem. Phys.* 1964, **40**, 2900
12 Clark, E. S. and Muus, L. T. *Z. Krist.* 1962, **117**, 119 and 108
13 Masetti, G., Cabassi, G. and Zerbi, G. *Macromolecules* 1973, **6**, 700
14 Clark, E. S. *J. Macromol. Sci. Phys.* 1967, **B1**, 795
15 DeSantis, P., Giglio, E., Liquori, A. M. and Ripamonte, A. *J. Polym. Sci.* 1963, **A1**, 1383
16 Martin, G. M. and Eby, R. K. *J. Res. Nat. Bur. Stand.* 1968, **72A**, 467
17 Hannon, M. J., Boerio, F. J. and Koenig, J. L. *J. Chem. Phys.* 1969, **50**, 2829
18 Corradini, P. and Guerra, G. *Macromolecules* 1977, **10**, 1410
19 Colson, J. P. and Eby, R. K. *J. Appl. Phys.* 1966, **37**, 3511
20 Bolz, L. H. and Eby, R. K. *J. Res. Nat. Bur. Stand.* 1965, **69A**, 481
21 Marx, P. and Dole, M. *J. Am. Chem. Soc.* 1955, **77**, 4771
22 Ishinabe, T. *Rep. Prog. Polym. Phys. Jpn* 1975, **18**, 167
23 Eby, R. K., Weeks, J. J., Farmer, B. L. and Sanchez, I. C. *Bull. Am. Phys. Soc.* 1976, **21**, 267. See also Eby, R. K., Sanchez, I. C. and Weeks, J. J. *International Microsymposium on the Crystallization & Fusion of Polymers,* Louvain, 1976, Preprints, 25
24 Akatsuka, Y., Noshiro, M. and Jitsugiri, Y. *Rep. Res. Lab. Asahi Glass Co. Ltd.* 1976, **26** (2), 111
25 *Thermal Analysis News Letter,* Perkin Elmer Corp. 1972, **10**, 1

Certain commercial materials and equipment are identified in order to specify adequately the experimental procedure. In no case does such identification imply recommendation or endorsement by the National Bureau of Standards, nor does it imply necessarily the best available for this purpose.

26 Ditmars, D. A. and Douglas, T. B. *J. Res. Nat. Bur. Stand.* 1971, **75A**, 401
27 Richardson, M. J. and Savill, N. G. *Thermochim. Acta* 1975, **12**, 213
28 Clark, E., Piermarini, G., Weeks, J., Block, S. and Eby, R. *Bull. Am. Phys. Soc.* 1979, **24**, 285 (to be published)
29 Sanchez, I. C. and Eby, R. K. *J. Res. Nat. Bur. Stand.* 1973, **77A**, 353
30 Sperati, C. A. and Starkweather, H. W. Jr. *Fortschr. Hochpolymforsch.* 1961, **2**, 465
31 Yasuda, T. and Araki, Y. *J. Appl. Polym. Sci.* 1961, **5**, 331
32 McCrum, N. G. *Makromol. Chem.* 1959, **34**, 50
33 Potts, R. B. *Proc. Comb. Phil. Soc.* 1952, **48**, 106
34 Golner, G. *Phys. Rev.* 1973, **B8**, 3419
35 Kim, D. and Joseph, R. I. *J. Phys. A.* 1975, **8**, 891
36 Enting, I. G. and Domb, C. *Ibid.* 1975, **8**, 1228
37 Sanchez, I. C., Colson, J. P. and Eby, R. K. *J. Appl. Phys.* 1973, **44**, 4332